

In silico ADME/T and 3D QSAR analysis of KDR inhibitors

S. M. Zahid Hosen^{1*}, Raju Dash¹, Mahmuda Khatun¹, Rasheda Akter¹, Md. Habibur Rahman Bhuiyan², Md. Rezaul Karim³, Nusrat Jahan Mouri⁴, Forkan Ahamed⁵, Kazi Saiful Islam⁶, Sadia Afrin⁷

¹Molecular Modeling & Drug Design Laboratory (MMDDL), Pharmacology Research Division, Bangladesh Council of Scientific & Industrial Research (BCSIR), Chittagong-4220, Bangladesh. ²Industrial Microbiology Research Division, Bangladesh Council of Scientific & Industrial Research (BCSIR), Chittagong-4220, Bangladesh. ³Institute of Food Science & Technology (IFST), BCSIR, Dhaka. ⁴Industrial Botany Research Division, Bangladesh Council of Scientific & Industrial Research (BCSIR), Chittagong-4220, Bangladesh. ⁵Department of Microbiology, Faculty of Biological Science, University of Chittagong, Chittagong, Bangladesh. ⁶Charles Perkins Center-University of Sydney, NSW 2050, Australia. ⁷Department of Nutritional Biochemistry, ICDDR, B, Dhaka 1212, Bangladesh.

ARTICLE INFO

Article history:

Received on: 16/08/2016

Revised on: 17/09/2016

Accepted on: 30/09/2016

Available online: 31/01/2017

Key words:

N-4-chlorophenylnaphthamides, QSAR, QSTR, HUMO, LUMO, LD₅₀, KDR

ABSTRACT

Tyrosine kinases (KDR) have been considered as a potential targets for the design of new anticancer agents. Recently, a series of N-4-chlorophenylnaphthamides has been reported with KDR inhibitory activity. In order to demonstrate the pharmacokinetics and the relationship between the structures and their inhibition of KDR, 3D-QSAR and *in silico* ADME/T analysis were performed on a dataset of 13 compounds. Quantum chemical parameters such as LUMO energy, HOMO energy, ionization energy (I), electron affinity (A), chemical potential (μ), hardness (η) and electrophilicity (χ) of the compounds are calculated by using semi-empirical SCF-MO method at PM3 level of theory and various SlogP descriptors from MOE software. *In silico* ADME/T analysis was performed by using different software's Discovery Studio 2.5, TOPKAT and QikProp 4.3. From *in silico* ADME and Toxicity studies, it was revealed that selected derivatives have good oral absorption rate and metabolism with no BBB penetration. QSTR (Quantitative Structure Toxicity Relationship) studies by using TOPAK in various computational animal models, showed high LD₅₀ values and the compounds are found to be noncarcinogenic. Moreover, three different QSAR models were generated by Partial Least Squares (PLS) Regression method having correlation coefficient (Q^2) of 0.86382, 0.84372, and 0.82629, respectively. These models conclude a significant relationship of KDR inhibition with dipole moment (D), LUMO energy (E_{LUMO}), hardness (η) and electrophilicity (χ), and hydrophobicity of compounds, regarding N-4-chlorophenylnaphthamides.

INTRODUCTION

New blood vessels formation from existing vasculature is termed as angiogenesis, a crucial pathway for tissue repair, growth and embryogenesis (Cherrington *et al.*, 2000, Ferrara, 2002, Harmange *et al.*, 2008) and associated with different types of pathological processes which include metastasis (Liotta *et al.*, 1991), tumor growth (Folkman, 1972), psoriasis (Detmar, 2000), ocular neovascularization (Aiello *et al.*, 1994), rheumatoid

arthritis (Walsh and Haywood, 2001), inflammation (Fava, 1994). Vascular endothelial growth factor (VEGF_a) and its receptor tyrosine kinases VEGFR-2 or kinase insert domain receptor (KDR) and VEGFR-1 were reported as key regulators for angiogenesis (Terman *et al.*, 1992). Briefly, downstream pathways are initiated by the accumulation of receptor dimerization and intercellular autophosphorylation, when VEGF binds with its receptor VEGFRs. As a corollary, vascular permeability, endothelial cell proliferation, survival and migration are increased and resulted in tumor growth and metastasis (Kilari *et al.*, 2013; Quentmeier *et al.*, 2012). Moreover, excessive expression of VEGFR is related to the poor prognosis and aggressiveness of the tumor in most of the cancers and therefore, inhibition of KDR-VEGF binding activity is

* Corresponding Author

S. M. Zahid Hosen, Molecular Modeling & Drug Design Laboratory (MMDDL), Pharmacology Research Division, Bangladesh Council of Scientific & Industrial Research (BCSIR), Chittagong-4220, Bangladesh. Email: smzahidhosen@bcsir.gov.bd

one of the major strategies in cancer drug development (Li *et al.*, 2016). Some successful strategies to inhibit the angiogenesis have been effectively expressed in preclinical and clinical layout. These approaches include VEGF soluble decoy receptors (Cardones and Banez, 2006), antibodies directed against VEGF (D'Adamo *et al.*, 2005), and small molecules that inhibit KDR (Adjei, 2007; Beebe *et al.*, 2003; Gingrich *et al.*, 2003; Harmange *et al.*, 2008; Hennequin *et al.*, 2002; Ruggeri *et al.*, 2003; Ryan and Wedge, 2005; Sun *et al.*, 2003; Thomas *et al.*, 2003). From these observations and ever increasing demands of these biological active KDR inhibitors, we subjected some novel N-4-chlorophenyl naphthamide based KDR inhibitors to study their QSAR and QSTR profiles.

The approach are used based on the popular quantum based drug design methodologies to describe the ADME/T profiles and activity by taking some quantum chemical parameters including dipole moment (D), LUMO energy (E_{LUMO}), hardness (η) and electrophilicity (χ), along with hydrophobic descriptor SLogP.

MATERIALS AND METHODS

Dataset preparation

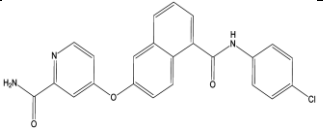
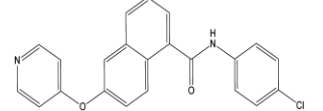
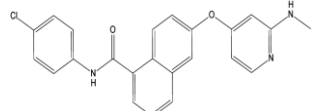
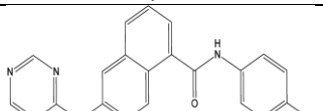
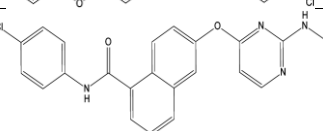
Thirteen N-4-chlorophenyl naphthamides with KDR inhibitory activity were used in systemic ADME/T and QSAR analysis are represented in **Table 1**. The molecules were drawn in Symyx Drawer and then subjected to generate 3D molecular structure by energy minimizing them with MMFF force field (Halgren, 1996) followed by considering distance-dependent

dielectric constant of 1.0 and convergence criterion of 0.01 kcal/mol A.

Prediction of ADME descriptors and toxicity

The major reason for the failure of most of the drug candidates during clinical trial are poor ADME and high toxicity profile. Thus an important aspect of drug discovery is to evaluate critical physico-chemical as well as toxicity profile in initial stages of drug discovery (Ray *et al.*, 2010). Hence, to select a potential drug candidate, all 13 hypothetical ligands were screened on the basis of ADME and toxicity filter using QikProp 4.3 from Schrodinger 2013 software. QikProp used Maestro-formatted .mae files (also known as 3D SD files) as input. Output of QikProp showed a number of principal descriptors and ADME properties as shown in **Table S1** (Choudhary *et al.*, 2015). Lipinski rule of 5 was applied on the ligands and hits which were having more than 1 violation were rejected. Various other physicochemical properties were also calculated, represented by different descriptors such as molar weight (MW), number of rotatable bonds (NRB), lipophilicity parameter [$\log P(o/w)$], number of hydrogen bond acceptors (HBA), number of hydrogen bond donors (HBD), total polar surface area (TPSA), solubility ($\log s$), solvent-accessible surface area (SASA), skin permeability ($\log Kp$), binding to human serum albumin ($\log K_{hsa}$), blood-brain partition coefficient ($\log BB$), apparent MDCK cell permeability (affyPMDCK), apparent Caco-2 cell permeability (affyPCaco), percentage human oral absorption (Dash *et al.*, 2015). Ideal ranges of various descriptors calculated with the reference to 95% of drugs are presented in **Table S1**.

Table 1: Descriptions and activity of the selected KDR inhibitors including name, structure and predicted activity by using three different models.

Compound Name	Structure	Compound's Name	IC ₅₀	pIC ₅₀			
				Observed	Cal (D, SLOGP, χ)	Cal (D, SLOGP, LUMO)	Cal (D, SLOGP, η)
1		4-(5-((4-Chlorophenyl)carbamoyl)naphthalen-2-yloxy)-N-methylpicolinamide	3	8.52288	8.27259	8.26322	8.13549
2		N-(4-Chlorophenyl)-6-(pyridin-4-yloxy)-1-naphthamide	5	7.74473	7.82488	7.92529	7.83936
3		N-(4-Chlorophenyl)-6-(2-(methylamino)pyridin-4-yloxy)-1-naphthamide	7	8.1549	7.72738	7.71313	7.89485
4		N-(4-Chlorophenyl)-6-(pyrimidin-4-yloxy)-1-naphthamide	310	6.50864	6.69023	6.59928	6.8149
5		N-(4-Chlorophenyl)-6-(2-(methylamino)pyrimidin-4-yloxy)-1-naphthamide	46	7.33724	7.81124	7.80144	7.73016

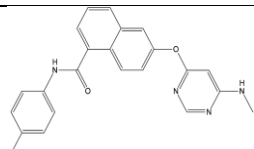
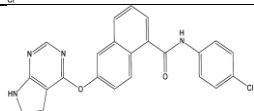
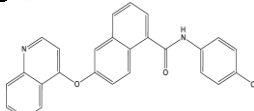
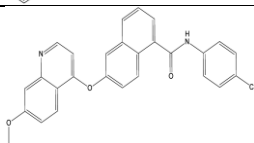
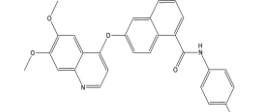
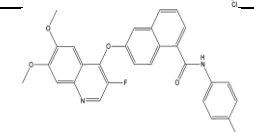
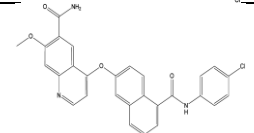
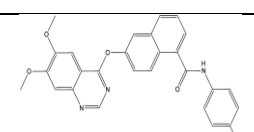
6		N-(4-Chlorophenyl)-6-(6-(methylamino)pyrimidin-4-yloxy)-1-naphthamide	20	7.69897	7.63951	7.66307	7.54596
7		6-(7H-Pyrrolo[2,3-d]pyrimidin-4-yloxy)-N-(4-chlorophenyl)-1-naphthamide	28	7.55284	7.54616	7.54635	7.54794
8		N-(4-Chlorophenyl)-6-(quinolin-4-yloxy)-1-naphthamide	4	8.39794	8.29596	8.46617	8.44174
9		N-(4-Chlorophenyl)-6-(7-methoxyquinolin-4-yloxy)-1-naphthamide	1	9	8.9622	8.61254	8.53581
10		N-(4-Chlorophenyl)-6-(6,7-dimethoxyquinolin-4-yloxy)-1-naphthamide	0.5	7.38722	7.85128	7.9445	7.94698
11		N-(4-Chlorophenyl)-6-(3-fluoro-6,7-dimethoxyquinolin-4-yloxy)-1-naphthamide	20	7.69897	7.71085	7.7105	7.70762
12		4-(5-((4-Chlorophenyl)carbamoyl)naphthalen-2-yloxy)-7-methoxyquinoline-6-carboxamide	0.2	9.69897	9.94529	9.95451	10.0802
13		N-(4-Chlorophenyl)-6-(6,7-dimethoxyquinazolin-4-yloxy)-1-naphthamide	2	8.69897	8.12471	8.20227	8.18124

Table S1: The Descriptors used in ADME-T prediction.

Predicted physicochemical properties	Used Descriptors	Ideal Range in 95% of drugs
Predicted molecular weight	MW	311–650
Predicted dipole moment	DM	0.000–1000.0
Predicted total molecular solvent accessible surface area	SASA	300.0–1000.0
Predicted hydrophobic SASA	FOSA	0–750
Predicted hydrophilic SASA	FISA	7–330
Predicted carbon Pi SASA	PISA	0–450
Predicted weakly polar SASA	WPSA	0–175
Predicted number of hydrogen bond donor	HB-donor	0–6
Predicted number hydrogen bond acceptor	HB-accept	2–20
Predicted octanol/gas partition coefficient	QP log P OCT	8.0–35.0
Predicted water/gas partition coefficient	QP log P W	4.0–45.0
Predicted octanol/water partition coefficient	QP log PO/W	–2–6.5
Predicted aqueous solubility	QP Log S	–6.5–0.5
Predicted blood–brain partition coefficient	QPLogBB (Cbrain/Cblood)	–3.0–1.2
Predicted skin permeability	QP Log KP	–8.0 to –1.0
Predicted van der Waals surface area of polar nitrogen and oxygen atoms	PSA	7–200
Predicted human oral absorption	HOA	>80% is high <25% is low
Predicted number of rotatable bond	#rotor	<10
Predicted ionization potential	IP(ev)	0.000–9.000
Predicted apparent MDCK cell permeability in nm/sec	AffyPMDCK	<25 poor, >500 great
Predicted apparent Caco-2 cell permeability in nm/sec	AffyPCaco	<25 poor, >500 great
Prediction of binding to human serum albumin.	QPLogKhsa	–1.5–1.5
Predicted IC ₅₀ <i>in vitro</i>	Log HERG	Concern below –5
Lipinski's rule of five	Rule of 5	Max 4

ADME/T prediction in Discovery Studio

For additional validation purpose, Discovery studio 2.5 (Accelrys, San Diego, CA, USA) was used to describe absorption, distribution, metabolism, elimination, and toxicity (ADME/T) properties by using ADME/T descriptors module. Based on the existing information of drug, six mathematical models are used in the modules to predict quantitatively the properties by a using set of rules/keys (**Table S2**) that specify threshold ADME/T characteristics for the chemical structure of the molecules. TOPKAT predictor was also selected, where the models that were used to calculate using TOPKAT are Rat Oral LD₅₀ (v3.1), Daphnia EC₅₀ (v3.1).

Table S2: ADMET descriptors and their rules/keys.

ADMET absorption level (human intestinal absorption)		
Level	Description	
0	Good absorption	
1	Moderate absorption	
2	Low absorption	
3	Very low absorption	
ADMET aqueous solubility level		
Level	Value	Description
0	$\log(\text{molar solubility}) < -8.0$	Extremely low
1	$-8.0 < \log(\text{molar solubility}) < -6.0$	No, very low, but possible
2	$-6.0 < \log(\text{molar solubility}) < -4.0$	Yes, low
3	$-4.0 < \log(\text{molar solubility}) < -2.0$	Yes, good
4	$-2.0 < \log(\text{molar solubility}) < 0.0$	Yes, optimal
5	$0.0 < \log(\text{molar solubility})$	No, too soluble
6	-1000	Warning: molecules with one or more unknown AlogP98 types
ADMET (blood brain barrier penetration level) BBB		
Level	Description	
0	Very High	
1	High	
2	Medium	
3	Low	
4	Undefined	
5	Warning: molecules with one or more unknown AlogP calculation	
Predictedclass	ADMET CYP2D6	
	Value	
0	Noninhibitor	
1	Inhibitor	
Predictedclass	ADMET hepatotoxicity	
	Value	
0	Nontoxic	
1	Toxic	
ADMET (plasma protein binding level) PPB		
Level	Description	
0	Binding is <90%	
1	Binding is ≥90%	
2	Binding is ≥95%	

Quantum Descriptors calculation and QSAR Analysis

All compounds were subjected to geometry optimization by using semi-empirical SCF-MO method, implemented in MOPAC 7.0. Here, basis set PM3 was used to calculate the

quantum descriptors. The following quantum chemical descriptors were considered: the energy of the highest occupied molecular orbital (E_{HOMO}), the lowest unoccupied molecular orbital (E_{LUMO}), the band gap energy (ΔE), the dipole moment (D), Electrophilicity (χ), Global Hardness (η). Using Koopmans' approximation, and ionization energy (I) and electron affinity (A) can be expressed in terms of the energies of the highest occupied (E_{HOMO}) and the lowest unoccupied molecular orbital (E_{LUMO}) as:

$$\begin{aligned} \text{Ionization potential, } I &= -E_{\text{HOMO}} \\ \text{Electron affinity, } A &= -E_{\text{LUMO}} \end{aligned}$$

Electrophilicity index is defined (χ) as a measure of the decrease in energy due to the maximal transfer of electrons from a donor to an acceptor system and is given as:

$$\chi = \mu/2\eta$$

Where, μ and η are the chemical potential and hardness, respectively. Chemical potential and hardness can be expressed in terms of ionization energy (I) and electron affinity (A) as given below:

$$\eta = [\text{HOMO}\epsilon - \text{LUMO}\epsilon]/2$$

$$\mu = \left(\frac{\partial E}{\partial N} \right)_{v(r)} \approx -\frac{I + A}{2}$$

After that, **2D molecular descriptors**, SlogPs (according to various subdivided accessible van der Waals surface area) were calculated by the program MOE (MOE software: Chemical computing group's molecular operating environment (MOE) software, version 2014.0901). After that, PLS QSAR (Geladi and Kowalski, 1986, Helland, 1988) analysis was performed to determine the relationship between these molecular descriptors and biological activity of the compounds. The maximum condition number of the principal component transform of the correlation matrix S , the condition limit, was set at 1.0×10^6 which is a very high setting. The leave-one-out cross validation (LOO-CV) scheme was used to validate the models and the correlation coefficient (Q^2) and root-mean-square error (RMSE) were reported.

RESULTS AND DISCUSSIONS

ADME and toxicity screening

All 13 hypothetical compounds were screened for "drug-likeness and "non-toxic" profile on the basis of various parameters of the software QikProp. ADME filter lead to 13 drugs like hits. The ADME prediction studies data of 13 hits are shown in **Table 2**. The range of various important parameters were predicted, like molecular weight lied in range between 374.826 and 502.928, the value of total solvent accessible surface area (SASA) ranged 645.681–802.389, estimated number of hydrogen

bonds donated (Donor HB) by the solute to water molecules in an aqueous solutions was found between 1 and 3, estimated number of hydrogen bonds accepted (accept HB) by the solute to water molecules in an aqueous solutions ranged 4–7.25, predicted octanol/gas par-tition coefficient (QlogPoct) ranged 18.439–27.16, predicted water/gas partition coefficient (QlogPw) ranged 10.268–16.232, predicted octanol/water partition coefficient (QlogPo/w) ranged 3.602–6.513, predicted aqueous solubility, log S (QlogS) ranged -5.684 to -8.177, predicted brain/blood partition coefficient (QlogBB) ranged -0.144 to -1.429, and Lipinski violations were ≤ 2 . Results of ADME-T studies reveal that compounds from **1** to **13** can be considered best, having druglikeliness as well as non-toxicity profile.

ADME/T Prediction by TOPAK

The use of *In silico* approaches to predict ADME/T properties is considered as a first step in the direction to analyze the new chemical entities to reduce wasting time on lead compounds which would be toxic or metabolized by the body into

an inactive form and unable to pass through membranes, and some results for this analysis are herein depicted in **Table 3** along with ADME/T descriptors and their rules/keys are tabulated in **Table S2**. The ADME/T profile of all the molecules under investigation was forecasted by means of six pre calculated ADME/T models provided by the Discovery Studio 2.5 program. Lipophilicity could be estimated as the log of the partition coefficient between n-octanol and water (logP). Though logP is generally used to determine a compound's lipophilicity, the fact that logP is a ratio creates a concern about the use of logP to score hydrophilicity and hydrophobicity (Hughes *et al.*, 2008). Thus the information of H-bonding prominences as obtained by calculating PSA could be taken into consideration along with logP calculation (Egan *et al.*, 2000). Therefore, a model with descriptors AlogP98 and PSA 2D were taken into consideration for the accurate prediction for the cell permeability of compounds. According to the model for a compound to have an optimum cell permeability should follow the evaluation criteria (PSA <140 Å² and AlogP98 <5) (Egan *et al.*, 2000).

Table 2: ADME-T descriptors of the compound calculated from QikProp.

Compound name	MW	SASA	HBD	HBA	Qlog Po/w	QlogS	QlogKp	QlogKhsa	AffyMDCK	Affy Caco-2	Qlog BB	QlogPoct	QlogPW	%HOA	PSA	Rule of 5
1	417.851	700.599	3	6.5	3.602	-5.99	-2.617	0.391	246.755	227.703	-1.389	23.459	15.402	90.23	105.509	0
2	374.826	651.13	1	4.5	4.956	-6.15	-0.588	0.672	2923.974	2242.509	-0.191	18.439	10.268	100	53.16	0
3	403.867	706.46	2	4.5	5.297	-6.844	-0.772	0.823	2502.012	1941.401	-0.359	21.084	11.383	100	64.318	1
4	375.813	645.681	1	5.5	4.22	-5.684	-1.219	0.435	1514.856	1220.398	-0.473	18.622	11.202	100	66.347	0
5	404.855	702.79	2	5.5	4.624	-6.457	-1.313	0.61	1424.41	1152.841	-0.617	21.138	12.327	100	76.818	0
6	404.855	692.903	2	5.5	4.443	-6.285	-1.702	0.597	940.088	784.881	-0.779	20.866	12.298	100	79.286	0
7	414.85	676.781	2	5	4.544	-6.327	-1.725	0.684	781.341	661.434	-0.768	20.965	12.461	100	80.817	0
8	424.885	715.766	1	4	6.121	-7.505	-0.195	1.124	3490.211	2641.573	-0.144	20.166	10.37	100	52.128	1
9	454.912	752.592	1	4.75	6.212	-7.719	-0.293	1.129	3503.646	2650.982	-0.218	21.12	10.597	100	60.396	1
10	484.938	797.04	1	5.5	6.396	-8.065	-0.37	1.171	3370.03	2557.287	-0.316	22.375	10.957	100	64.821	1
11	502.928	794.337	1	5.5	6.513	-8.177	-0.509	1.181	5373.213	2559.34	-0.219	22.273	10.694	100	65.178	2
12	497.937	802.389	3	7.25	4.694	-7.321	-2.217	0.737	329.67	297.696	-1.429	27.16	16.232	100	110.338	0
13	485.926	789.7	1	6.5	5.682	-7.535	-0.828	0.908	2117.295	1663.539	-0.535	22.446	11.875	100	78.508	1

Data indicate the descriptor calculated from QIKProp 4.3, where each descriptor represent one physicochemical properties for “druglikeliness” such as MW- molecular weight; SASA- Solvent Assessable Surface Area; HBD- no. of H bond donor; HBA- no. of H bond acceptor; QlogPo/w- predicted octanol/water partition coefficient; QlogS- predicted aqueous solubility; QlogKp- predicted skin permeability; QlogKhsa- predicted human serum albumin binding; Affy MDCK- Apparent MDCK cell permeability; AffyCaco- Apparent Caco-2 cell permeability; QlogBB- predicted brain/blood partition coefficient; QlogPoct- predicted octanol/gas partition coefficient; QlogPw- predicted water/gas partition coefficient. %HOA- Percentage Human Oral Absorption; PSA- Total Polar Surface Area; Rule of 5- Lipinski violations.

Table 3: Computer aided ADME/T screening Of 13 Compounds.

Compound Name	ADME/T absorption level	ADME/T AlogP98	ADME/T unknown AlogP98	ADME/T PSA 2D	ADME/T BBB level	ADME/T BBB	ADME/T solubility	ADME/T solubility level	ADME/T hepatotoxicity	ADME/T hepatotoxicity probability	ADME/T CYP2D6	ADME/T CYP2D6 probability	ADME/T PPB level
1	0	4.027	0	94.142	4	-	-5.842	2	1	0.986	0	0.465	1
2	0	4.597	0	50.302	4	-	-5.966	2	1	0.98	1	0.712	2
3	0	4.944	0	63.112	1	0.376	-6.28	1	1	0.986	1	0.673	1
4	0	4.508	0	61.563	1	0.265	-5.967	2	1	0.98	1	0.722	2
5	0	4.837	0	74.373	1	0.164	-6.349	1	1	0.98	1	0.712	2
6	0	4.855	0	74.373	1	0.17	-6.365	1	1	0.98	1	0.712	2
7	0	4.861	0	76.618	1	0.136	-6.834	1	1	0.986	1	0.594	1
8	1	5.934	0	50.302	0	0.884	-7.494	1	1	0.986	1	0.574	2
9	1	5.917	0	59.232	0	0.738	-7.375	1	1	0.986	1	0.564	2
10	1	5.901	0	68.162	4	-	-7.268	1	1	0.973	1	0.603	2
11	1	6.106	0	68.162	4	-	-7.444	1	1	0.98	1	0.653	2
12	1	4.919	0	103.072	4	-	-6.915	1	1	0.98	1	0.603	1
13	1	5.812	0	79.423	4	-	-7.247	1	1	0.973	1	0.554	2

Table 4: Rat oral LD₅₀- Rat oral lethal dose 50

Compound Name	Rat Oral LD ₅₀ Heteroaromatic Model	
	Computed Rat Oral LD ₅₀	95% Confidence Limits
1	476.9 mg/kg	75.1 mg/kg & 3 g/kg
2	478.7 mg/kg	79.6 mg/kg & 2.8 g/kg
3	504.1 mg/kg	85 mg/kg & 3 g/kg
4	474.5 mg/kg	81.6 mg/kg & 2.8 g/kg
5	595.2 mg/kg	101.5 mg/kg & 3.5 g/kg
6	576.9 mg/kg	98 mg/kg & 3.4 g/kg
7	404 mg/kg	68.9 mg/kg & 2.4 g/kg
8	341.1 mg/kg	57.5 mg/kg & 2 g/kg
9	297 mg/kg	50 mg/kg & 1.8 g/kg
10	139 mg/kg	22.8 mg/kg & 848 mg/kg
11	312.5 mg/kg	51.6 mg/kg & 1.9 g/kg
12	229.2 mg/kg	35 mg/kg & 1.5 g/kg
13	161.4 mg/kg	26.6 mg/kg & 980.8 mg/kg

Table 5: Daphnia EC₅₀ – Daphnia effective concentration 50

Compound Name	Model: Daphnia EC ₅₀ (v3.1)	
	Computed EC ₅₀ values	95% Confidence Limits
1	5.4ug/l	731.1ng/l&39.2ug/l
2	10.6 ug/l	1.8 ug/l&1.9mg/l
3	347.5ug/l	58.1ug/l&2.1mg/l
4	13.6ug/l	2.2ug/l&83.2ug/l
5	299.5ug/l	50ug/l&1.8mg/l
6	325.7ug/l	54.5ug/l&1.9mg/l
7	21.9ug/l	3.3ug/l&146.3ug/l
8	25.4ug/l	3.7ug/l&175.8ug/l
9	165.1ug/l	24.3ug/l&1.1mg/l
10	19.6ug/l	2.5ug/l&152.2ug/l
11	1.8ug/l	204.5ng/l&16.3ug/l
12	43.3ug/l	5.3ug/l&352.8ug/l
13	18.8ug/l	2.4ug/l&146.1ug/l

All the compounds showed polar surface area (PSA) <140 Å². Considering the AlogP98 criteria, all inhibitors had AlogP98 value <5. **Table 2** shows that among 13 compounds, 6 compounds have undefined values for BBB penetration levels (4 as mentioned in **Table 2**) with the exception of 7 compound having very high and high value (level 0 and 1) BBB penetration level. The aqueous solubility plays an essential role in the bioavailability of the candidate, all of them having low aqueous solubility level shown as **Table S2**.

All compounds have been predicted to have hepatotoxicity level of 1 which is toxic to liver and lower rate of first pass metabolism. All compounds exhibit as an inhibitors with respect to CYP2D6 liver (with reference to **Table S1**) except compound **1** shown in **Table 3**.

This indicates that they are less metabolized in Phase-I metabolism except one. Finally, the ADME/T plasma protein binding property prediction denotes that for compounds **1, 2, 3, 7, 12** binding is ≥90% and rest of them binding is ≥95% respectively, (refer to **Table S1**), clearly suggesting that all of them have good bioavailability and are not likely to be highly bound to carrier proteins in the blood. The Rat Oral LD₅₀ values of all the compounds are within the Optimum Prediction Space (OPS). And the LD₅₀ values are satisfactory. These high LD₅₀ values indicate higher safety of these compounds (**Table 4**). The values obtained from daphnia EC₅₀ model show remarkable EC₅₀ values (**Table 5**).

QSAR models for inhibitor activity

The quantum chemical descriptors calculation that obtained from geometry optimization like, dipole moment, HOMO energy, LUMO energy, ionization energy, electron affinity, chemical potential, hardness, and electrophilicity of thirteen molecules are represented in **Table S3**. Parameters like dipole moment, LUMO energy, hardness and electrophilicity were considered to predict model, since these parameters are widely used to describe the stability, toxicity and reactivity of the chemical compounds (Kapur *et al.*, 2000). We also considered the hydrophobicity, as many authors reported the quantitative correlation of toxicity, activity and metabolism of the compounds with the octanol-water distribution coefficient descriptor (Bundy *et al.*, 2001, Ren and Frymier, 2002, Worgan *et al.*, 2003). In order to establish a better predictability, PLS based QSAR study was performed by considering experimentally observed values (pIC₅₀), along with various descriptors, are presented in **Tables 1**. According to the analysis, the best model included the following predictors: SLogP, dipole moment (D), and electrophilicity (χ). The model is expressed in the **Eq. 1**.

$$pIC_{50} = -6.21625 + 0.18964(D) + 0.55132(\chi) + 0.05674(SlogP_VSA9) + 0.00000(SlogP_VSA8) + 0.01887(SlogP_VSA7) + 0.00000(SlogP_VSA6) + 0.02588(SlogP_VSA5) + 0.20657(SlogP_VSA4) +$$

$$0.00000(\text{SlogP_VSA3}) + 0.00408(\text{SlogP_VSA2}) + 0.01233(\text{SlogP_VSA1}) - 0.12129(\text{SlogP_VSA0}) + 0.00522(\text{SlogP})$$

n=	Q ² =	RMSE=	R ² _{crossvalidated} =	RMSE _{cross validated} =
13	0.86382	0.29494	0.01642	13.70550

The model considers the higher contributions of SLogP, dipole moment (D) and electrophilicity (χ) with inhibitory activity. A plot of the predicted activity versus experimental activity for molecules using training set for model of KDR inhibition is shown in **Figure 1**.

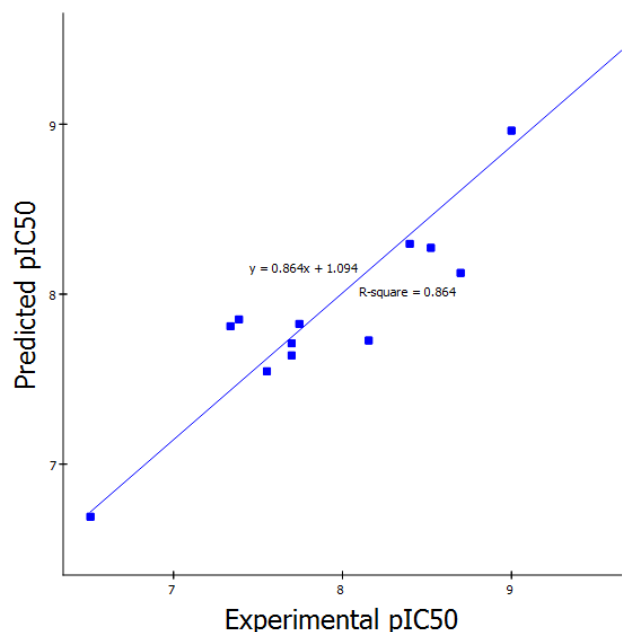


Fig. 1: Calculated and observed activity using SLogP, dipole moment (D), and electrophilicity (χ) descriptors.

Regarding these descriptors, another best model was observed in case of LUMO energy, in conjunction with Dipole moment (D) and SLogP. The plot of predicted activity values (pIC_{50}) versus that predicted on the basis of regression equation for a complete set of inhibitors is presented in **Figure 2**.

$$\text{pIC}_{50} = -7.88749 + 0.07002(\text{SlogP_VSA9}) + 0.00000(\text{SlogP_VSA8}) + 0.02555(\text{SlogP_VSA7}) + 0.00010(\text{SlogP_VSA6}) + 0.21801(\text{SlogP_VSA4}) + 0.03065(\text{SlogP_VSA5}) + 0.00000(\text{SlogP_VSA3}) - 0.19162(\text{SlogP}) - 0.13445(\text{SlogP_VSA}) + 0.01493(\text{SlogP_VSA1}) + 0.01656(\text{SlogP_VSA2}) + 0.18532(\text{D}) - 3.23828(\text{LUMO})$$

n=	Q ² =	RMSE=	R ² _{crossvalidated} =	RMSE _{cross validated} =
13	0.84372	0.31595	0.01635	13.99739

The contribution of global hardness (η) was also found in the correlation of biological activity, along with dipole moment (D) and SlogP, which is shown in **eq. (3)**. The correlations that found in **eq. 3**, is rendered in **Figure 3**.

$$\text{pIC}_{50} = -4.02472 - 0.00333(\eta) + 0.18400(\text{D}) + 0.00704(\text{SlogP}) - 0.00286(\text{SlogP_VSA1}) - 0.11944(\text{SlogP_VSA0}) - 0.00287(\text{SlogP_VSA2}) + 0.00000(\text{SlogP_VSA3}) + 0.20603(\text{SlogP_VSA4}) + 0.00000(\text{SlogP_VSA6}) + 0.02992(\text{SlogP_VSA5}) + 0.01952(\text{SlogP_VSA7}) + 0.00000(\text{SlogP_VSA8}) + 0.03195(\text{SlogP_VSA9})$$

n=	Q ² =	RMSE=	R ² _{crossvalidated} =	RMSE _{cross validated} =
13	0.82629	0.33310	0.02219	10.80850

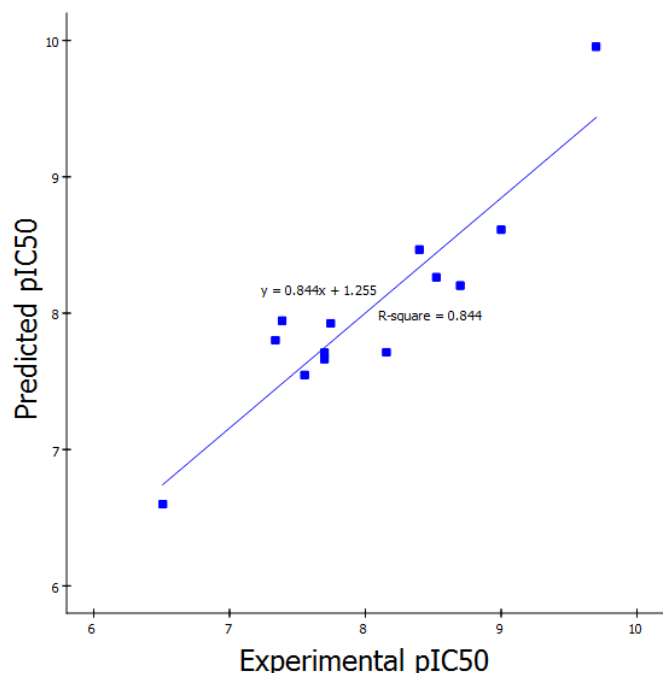


Fig. 2: Observed and calculated pIC_{50} values using SLogP, dipole moment (D), and E_{LUMO} energy descriptors.

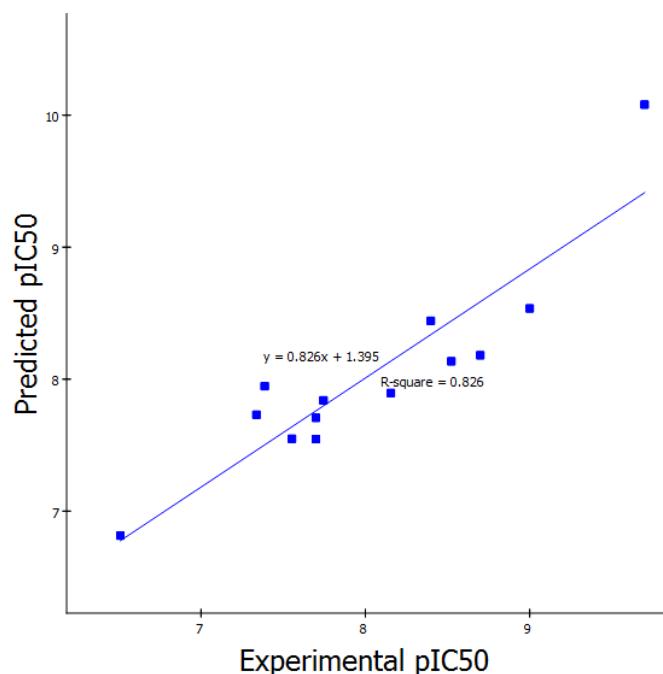


Fig. 3: Observed and calculated pIC_{50} values using SLogP, dipole moment (D), and hardness (η) descriptors.

Table S3: Calculated quantum descriptors of selected KDR inhibitors.

Compound Name	Dipole Moment (D)	HOMO (E_{HOMO})	LUMO (E_{LUMO})	HOMO-LUMO GAP	Ionization potential (I)	Electron Affinity (A)	Global Hardness (η)	Ch. Potential (μ)	Electrophilicity (χ)
1	1.07	-0.326	-0.2443	0.08162	0.326	0.24438	0.04081	0.28519	0.996487823
2	5.97	-0.3306	-0.2275	0.1031	0.3306	0.2275	0.05155	0.27905	0.755275485
3	2.77	-0.3197	-0.0471	0.27261	0.31976	0.04715	0.136305	0.183455	0.123457456
4	2.68	-0.3235	-0.0450	0.27852	0.32354	0.04502	0.13926	0.18428	0.121927037
5	4.18	-0.3160	-0.0383	0.27768	0.31601	0.03833	0.13884	0.17717	0.113040942
6	3.15	-0.3254	-0.0486	0.27679	0.32545	0.04866	0.138395	0.187055	0.126411984
7	6.44	-0.3234	-0.0351	0.28833	0.32343	0.0351	0.144165	0.179265	0.111455416
8	4.91	-0.3254	-0.2043	0.12106	0.32542	0.20436	0.06053	0.26489	0.579602776
9	7.83	-0.2739	-0.2342	0.03973	0.27393	0.2342	0.019865	0.254065	1.624692279
10	7.04	-0.3322	-0.2248	0.10742	0.33229	0.22487	0.05371	0.27858	0.722461519
11	5.15	-0.3189	-0.0387	0.28028	0.31898	0.0387	0.14014	0.17884	0.114113549
12	9.28	-0.2677	-0.1722	0.09552	0.26776	0.17224	0.04776	0.22	0.506700168
13	10.59	-0.3314	-0.1400	0.19139	0.33141	0.14002	0.095695	0.235715	0.290305456

Studies relating the molecular properties of the compounds and their KDR inhibitory activity supported this hypothesis, as the descriptor dipole moment and SLogP show the higher contribution to the activity against KDR in the QSAR model, where contribution of electrophilicity is more significant than other descriptors. The higher LUMO energy is correlated with higher electron affinity. Henceforth, it concludes that increasing of electron affinity can increase the KDR inhibition activity. It is remarkable to note that increase in global hardness of the molecule leads to increase in stability and decrease in reactivity of the species (Ayers and Parr, 2000). From eq. (3), it also confirms that hardness of these molecules influence their inhibitory activity. However as a whole, this result is anticipated as the hydrophobicity and lipophilicity of the chemical compounds mainly govern their biological actions at cellular and molecular levels.

CONCLUSION

The current study is designed to reveal the therapeutic potentiality of some selected N-4-chlorophenyl naphthamide derivatives regarding the perspectives in tyrosine kinase inhibitor. In collateral, our findings agree with the existing evidence with concluding a better pharmacokinetics profile. The results of QSAR and ADME/T studies are validated each other and the developed mathematical models could provide insight into the structural requirements for the synthesis of new potential chemical structure having a better KDR inhibition activity.

Financial support and sponsorship: Nil.

Conflict of Interests: There are no conflicts of interest.

REFERENCES

Adjei AA. Novel small-molecule inhibitors of the vascular endothelial growth factor receptor. *Clinical lung cancer*. 2007;8:S74-S8.
 Aiello LP, Avery RL, Arrigg PG, Keyt BA, Jampel HD, Shah ST, et al. Vascular endothelial growth factor in ocular fluid of patients with diabetic retinopathy and other retinal disorders. *New England Journal of Medicine*. 1994;331(22):1480-7.

Ayers PW, Parr RG. Variational principles for describing chemical reactions: the Fukui function and chemical hardness revisited. *Journal of the American Chemical Society*. 2000;122(9):2010-8.

Beebe JS, Jani JP, Knauth E, Goodwin P, Higdon C, Rossi AM, et al. Pharmacological characterization of CP-547,632, a novel vascular endothelial growth factor receptor-2 tyrosine kinase inhibitor for cancer therapy. *Cancer research*. 2003;63(21):7301-9.

Bundy JG, Morriss AW, Durham DG, Campbell CD, Paton GI. Development of QSARs to investigate the bacterial toxicity and biotransformation potential of aromatic heterocyclic compounds. *Chemosphere*. 2001;42(8):885-92.

Cardones AR, Banez LL. VEGF inhibitors in cancer therapy. *Current pharmaceutical design*. 2006;12(3):387-94.

Cherrington JM, Strawn LM, Shawver LK. New paradigms for the treatment of cancer: the role of anti-angiogenesis agents. *Advances in cancer research*. 2000;79:1-38.

Choudhary D, Gupta GK, Khokra SL. Structure based designing and ADME-T studies of butenolide derivatives as potential agents against receptor ICAM-1: A drug target for cerebral malaria. *Journal of Computational Science*. 2015;10:156-65.

D'Adamo DR, Anderson SE, Albritton K, Yamada J, Riedel E, Scheu K, et al. Phase II study of doxorubicin and bevacizumab for patients with metastatic soft-tissue sarcomas. *Journal of Clinical Oncology*. 2005;23(28):7135-42.

Dash R, Hosen S, Karim M, Kabir MSH, Hossain MM, Junaid M, et al. In silico analysis of indole-3-carbinol and its metabolite DIM as EGFR tyrosine kinase inhibitors in platinum resistant ovarian cancer vis a vis ADME/T property analysis. *J App Pharm Sci*, 2015; 5 (11): 073-078.

Detmar M. The role of VEGF and thrombospondins in skin angiogenesis. *Journal of dermatological science*. 2000;24:S78-S84.

Egan WJ, Merz KM, Baldwin JJ. Prediction of drug absorption using multivariate statistics. *Journal of medicinal chemistry*. 2000;43(21):3867-77.

Fava GA. Affective disorders and endocrine disease: new insights from psychosomatic studies. *Psychosomatics*. 1994;35(4):341-53.

Ferrara N. VEGF and the quest for tumour angiogenesis factors. *Nature Reviews Cancer*. 2002;2(10):795-803.

Folkman J. Anti-angiogenesis: new concept for therapy of solid tumors. *Annals of surgery*. 1972;175(3):409.

Geladi P, Kowalski BR. Partial least-squares regression: a tutorial. *Analytica chimica acta*. 1986;185:1-17.

Gingrich DE, Reddy DR, Iqbal MA, Singh J, Aimone LD, Angeles TS, et al. A new class of potent vascular endothelial growth factor receptor tyrosine kinase inhibitors: structure-activity relationships for a series of 9-alkoxymethyl-12-(3-hydroxypropyl) indeno [2, 1-a] pyrrolo [3, 4-c] carbazole-5-ones and the identification of CEP-5214 and its dimethylglycine ester prodrug clinical candidate CEP-7055. *Journal of medicinal chemistry*. 2003;46(25):5375-88.

Halgren TA. Merck molecular force field. I. Basis, form, scope, parameterization, and performance of MMFF94. *Journal of computational chemistry*. 1996;17(5-6):490-519.

Harmange J-C, Weiss MM, Germain J, Polverino AJ, Borg G, Bready J, et al. Naphthamides as Novel and Potent Vascular Endothelial Growth Factor Receptor Tyrosine Kinase Inhibitors: Design, Synthesis, and Evaluation. *Journal of medicinal chemistry*. 2008;51(6):1649-67.

Helland IS. On the structure of partial least squares regression. *Communications in statistics-Simulation and Computation*. 1988; 17(2): 581-607.

Hennequin LF, Stokes ES, Thomas AP, Johnstone C, Plé PA, Ogilvie DJ, et al. Novel 4-anilinoquinazolines with C-7 basic side chains: design and structure activity relationship of a series of potent, orally active, VEGF receptor tyrosine kinase inhibitors. *Journal of medicinal chemistry*. 2002; 45(6): 1300-12.

Hughes LD, Palmer DS, Nigsch F, Mitchell JB. Why are some properties more difficult to predict than others? A study of QSPR models of solubility, melting point, and Log P. *Journal of chemical information and modeling*. 2008; 48(1): 220-32.

Kapur S, Shusterman A, Verma RP, Hansch C, Selassie CD. Toxicology of benzyl alcohols: a QSAR analysis. *Chemosphere*. 2000;41(10):1643-9.

Kilari S, Remadevi I, Zhao B, Pan J, Miao R, Ramchandran R, et al. Endothelial Cell-specific Chemotaxis Receptor (ECSCR) Enhances Vascular Endothelial Growth Factor (VEGF) Receptor-2/Kinase Insert Domain Receptor (KDR) Activation and Promotes Proteolysis of Internalized KDR. *The Journal of Biological Chemistry*. 2013; 288(15): 10265-74.

Li M-y, Lv Y-c, Tong L-j, Peng T, Qu R, Zhang T, et al. DW10075, a novel selective and small-molecule inhibitor of VEGFR, exhibits antitumor activities both in vitro and in vivo. *Acta Pharmacologica Sinica*. 2016;37(3):398-407.

Liotta LA, Steeg PS, Stetler-Stevenson WG. Cancer metastasis and angiogenesis: an imbalance of positive and negative regulation. *Cell*. 1991;64(2):327-36.

Quentmeier H, Eberth S, Romani J, Weich HA, Zaborski M, Drexler HG. DNA methylation regulates expression of VEGF-R2 (KDR) and VEGF-R3 (FLT4). *BMC Cancer*. 2012;12:19-.

Ray S, Madrid PB, Catz P, LeValley SE, Furniss MJ, Rausch LL, et al. Development of a new generation of 4-aminoquinoline antimalarial compounds using predictive pharmacokinetic and toxicology models. *Journal of medicinal chemistry*. 2010;53(9):3685-95.

Ren S, Frymier PD. Estimating the toxicities of organic chemicals to bioluminescent bacteria and activated sludge. *Water research*. 2002;36(17):4406-14.

Ruggeri B, Singh J, Gingrich D, Angeles T, Albom M, Chang H, et al. CEP-7055 A Novel, Orally Active Pan Inhibitor of Vascular Endothelial Growth Factor Receptor Tyrosine Kinases with Potent Antiangiogenic Activity and Antitumor Efficacy in Preclinical Models. *Cancer research*. 2003;63(18):5978-91.

Ryan A, Wedge S. ZD6474—a novel inhibitor of VEGFR and EGFR tyrosine kinase activity. *British journal of cancer*. 2005;92:S6-S13.

Sun L, Liang C, Shirazian S, Zhou Y, Miller T, Cui J, et al. Discovery of 5-[5-fluoro-2-oxo-1, 2-dihydroindol-(3 Z)-ylidenemethyl]-2, 4-dimethyl-1 H-pyrrole-3-carboxylic acid (2-diethylaminoethyl) amide, a novel tyrosine kinase inhibitor targeting vascular endothelial and platelet-derived growth factor receptor tyrosine kinase. *Journal of medicinal chemistry*. 2003;46(7):1116-9.

Terman BI, Dougher-Vermazen M, Carrion ME, Dimitrov D, Armellino DC, Gospodarowicz D, et al. Identification of the KDR tyrosine kinase as a receptor for vascular endothelial cell growth factor. *Biochemical and biophysical research communications*. 1992; 187(3): 1579-86.

Thomas AL, Morgan B, Dreves J, Unger C, Wiedenmann B, Vanhoefer U, et al., editors. Vascular endothelial growth factor receptor tyrosine kinase inhibitors: PTK787/ZK 222584. *Seminars in oncology*; 2003: Elsevier.

Walsh D, Haywood L. Angiogenesis: a therapeutic target in arthritis. *Current opinion in investigational drugs (London, England: 2000)*. 2001;2(8):1054-63.

Worgan AD, Dearden JC, Edwards R, Netzeva TI, Cronin MT. Evaluation of a Novel Short-Term Algal Toxicity Assay by the Development of QSARs and Inter-Species Relationships for Narcotic Chemicals. *QSAR & Combinatorial Science*. 2003;22(2):204-9.

How to cite this article:

Hosen SMZ, Dash R, Khatun M, Akter R, Bhuiyan MHR, Karim MR, Mouri NJ, Ahmed F, Islam KS, Afrin S. In silico ADME/T and 3D QSAR analysis of KDR inhibitors. *J App Pharm Sci*, 2017; 7 (01): 120-128.